

Low Fuel Convergence Path to Direct-Drive Fusion Ignition

Kim Molvig,^{1,2} Mark J. Schmitt,¹ B. J. Albright,¹ E. S. Dodd,¹ N. M. Hoffman,¹ G. H. McCall,¹ and S. D. Ramsey¹

¹Los Alamos National Laboratory, Los Alamos, New Mexico 87545, USA

²Massachusetts Institute of Technology, Cambridge, Massachusetts 02139, USA

(Received 19 February 2016; revised manuscript received 31 May 2016; published 24 June 2016)

A new class of inertial fusion capsules is presented that combines multishell targets with laser direct drive at low intensity (2.8×10^{14} W/cm²) to achieve robust ignition. The targets consist of three concentric, heavy, metal shells, enclosing a volume of tens of μg of liquid deuterium-tritium fuel. Ignition is designed to occur well “upstream” from stagnation, with minimal pusher deceleration to mitigate interface Rayleigh-Taylor growth. Laser intensities below thresholds for laser plasma instability and cross beam energy transfer facilitate high hydrodynamic efficiency ($\sim 10\%$).

DOI: 10.1103/PhysRevLett.116.255003

A large convergence ratio and high implosion velocity have been the hallmarks of inertial fusion from its inception [1,2]. Target design has evolved over the past forty-plus years to culminate in the National Ignition Facility (NIF) ignition targets fired during the Ignition Campaign of 2009–2012. These targets sought to ignite a central hot spot formed by a small fraction of fuel that could be heated to ignition temperatures. Burn was then projected to propagate to the main fuel and produce high gain. A specific example (Fig. 107 of Ref. [2]) composed entirely of light materials is driven by 1.35 MJ of laser light. It required an implosion velocity $u_I = 41$ cm/ μs and convergence ratio (initial capsule radius, R_i divided by final radius R_f) of $C = 36$ from a plastic and deuterium-tritium (DT) ice shell with an in-flight aspect ratio of 40. The predicted yield of 15 MJ from 180 μg of DT fuel corresponds to a burn fraction of 25%. Nearly perfect spherical symmetry was essential. The experimental results achieved to date on the NIF have underperformed predictions [3,4].

A fundamentally different path to ignition is described in this Letter. A new class of targets capable of producing multi-megajoule yields from DT fuel masses of tens of μg , absorbed drive energies less than 2 MJ, and burn fractions exceeding 50% is defined. High gain is abandoned as a goal. Instead, we seek a mechanically robust implosion and large margin for ignition. The Revolver targets described here consist of three nested, spherical metal shells with buffer gas between the shells and a central volume filled with cryogenic liquid DT fuel. The baseline target is depicted in Fig. 1, which also shows the implosion diagram from a HYDRA [5] 1D simulation (one in four zones plotted). Energy is absorbed by an ablator shell from a short laser pulse that leaves 70% of the ablator mass as payload to implode the target. The implosion is entirely mechanical, dominated by the metal shells. The metal multishell system is intended to be more robust hydrodynamically than a single plastic-DT ice shell. Ignition well upstream of stagnation is a key feature of the

Revolver targets. This is controlled with a design parameter that allows for adjustment of the ignition margin.

All the physics pieces we will assemble have long been known and studied. Metal pushers were first discussed in the literature by Kirkpatrick and co-workers [6,7], who showed the benefits of radiation trapping in reducing implosion velocities to $u_I \lesssim 20$ cm/ μs and ignition temperatures to $T_I \sim 2.5$ keV. The work continued with additional collaborators [8–11] who termed the configuration equilibrium ignition. Colgate and co-workers proposed a fusion concept based on velocity multiplication of nested cylindrical metal shells [12,13]. More recently, Amendt and collaborators advanced designs of the double-shell targets with one metal (pusher) shell for the NIF [14,15]. Laser

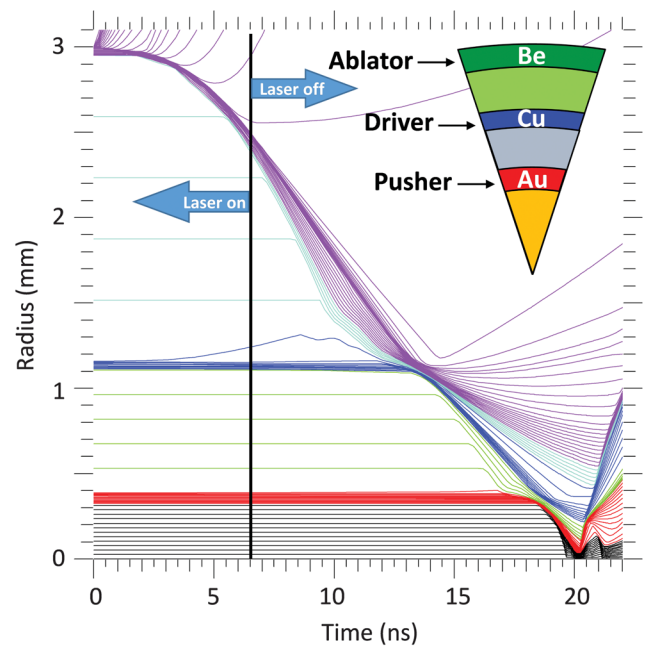


FIG. 1. Baseline Revolver capsule showing material pie chart and implosion diagram from 1D simulation (one in four zones plotted).

direct drive of such multishell systems described here is a novel concept.

The present Letter combines these physics elements into a complete model that clearly displays the physics differences. Complete specifications for the two inner shells and the laser and ablator requirements are given from this simple model as analytic functions of the pusher mass. The ablator shell design is found using HYDRA [5] code simulations.

The main features of this class of targets are (1) low convergences throughout, $C < 3$ for each shell collision, fuel convergence $C \sim 9$, (2) upstream ignition with minimal deceleration controlled by very large pusher–fuel mass ratio, and (3) the implosion velocity and convergence being reciprocally related, $u_I \propto C^{-1}$.

Convergence is small for all three shells. The system net convergence C_{net} , initial ablator outer radius divided by final fuel compressed radius, is large—a characteristic of all inertial confinement fusion (ICF) capsules. This leads to stringent requirements on drive uniformity [2]. For single-shell targets there is no remedy other than superb target and drive symmetry. For multishell targets, refreshment of symmetric mass at each collision and multiple shock reflections in the intervening low-density gas between shells can potentially be used to mitigate convergence amplification of asymmetries.

A simplified physics model is used to capture the average system behavior. The mass of fusion fuel that has been compressed and heated to ignition uniformly in a spherical volume is

$$M_{\text{DT}} = \frac{4\pi (\rho R)_I^3}{3\rho_0^2 C^6}, \quad (1)$$

where ρ_0 is the initial fuel density (set by technological constraints on manufacturing and assembly), $(\rho R)_I$ is the fuel areal density at ignition, and $C = R_0/R$ is the convergence ratio of the fuel. We use the current NIF capability for cryogenic liquid DT (at 33 K) of $\rho_0 \approx 0.173 \text{ g/cm}^3$ to set the initial fuel density. Requiring robust alpha self-heating sets the areal density as a design parameter taken here to be $(\rho R)_I \approx 0.5 \text{ g/cm}^2$. Having fixed $(\rho R)_I$ and ρ_0 as constraints, one is left with the relation between fuel mass and convergence $M_{\text{DT}} = 17.5C^{-6} \text{ g}$. Convergence is not independent from mass, but is constrained by this relation for an implosion that achieves the specified $(\rho R)_I$.

The implosion dynamics of the fuel has two hydrodynamic phases: a shock-heating phase, lasting until the shock converges on the origin, and a subsequent isentropic compression phase that heats the fuel to ignition temperature T_I . The behavior is similar to that of an ideal, spherical piston with constant implosion velocity. The average isentropic behavior of the second phase has been verified in simulations and shown to be valid despite the multiple weak shock reflections reverberating through the fuel evident in

the implosion diagram. Radiative losses are reduced by the metal pusher to a low level and are ignored in the simple model. The shock-heating phase heats the fuel to a temperature scaling with the square of the implosion velocity $T_* \propto u_I^2$. The strongly shocked fuel has equal kinetic and internal energy components, so (ignoring spherical geometry effects) $\frac{1}{2}\rho_* u_I^2 = 3n_* T_* = 3\rho_*(N_A/A)T_*$, or

$$u_I^2 = \frac{6N_A}{A} T_* = 2304T_*, \quad (2)$$

with numerical values for temperature in keV and velocity in cm/ μs , and assumed equimolar DT fuel. Convergence in pusher radius at the time of shock collapse t_* is a fundamental constant of the spherical piston problem. It is a property of the Euler equations and can be computed numerically [16]. This convergence value $C(t_*) \equiv C_*$ has the value $C_* \equiv R_0/R_S = 2.5$ (actually the convergence at time of peak fuel entropy). For times $t > t_*$ the compression is adiabatic, and the temperature rises with convergence as $T_I = T_* C^2/C_*^2$. The implosion velocity is

$$u_I = \left(\frac{6N_A}{A}\right)^{1/2} \frac{C_*}{C} T_I^{1/2} = 48 \frac{C_*}{C} T_I^{1/2}. \quad (3)$$

For $C = 10$ and corresponding ignition temperature $T_I = 2.5 \text{ keV}$, this gives $u_I = 19 \text{ cm}/\mu\text{s}$. The inferred shock temperature is $T_* = 156 \text{ eV}$.

Note that implosion velocity and convergence are inversely related. This property runs contrary to the traditional ICF principle that large implosion velocity is a virtue. It is not without some precedent (a more complex variant of this scaling is embedded in the ignition threshold factor of Lindl *et al.* [4]). For the Revolver capsule this behavior is a consequence of the negligible radiation losses and constant implosion velocity that come from the high density heavy metal pusher (compressed to over 2000 g/cm^3). An increase in implosion velocity increases the shock-heating temperature and causes the ignition temperature to be reached at lower convergence. If there is no commensurate increase in fuel mass to match the lower convergence, reduced burn performance will result. This dynamic can be observed in the simulations—faster implosion is not always better.

Revolver targets are designed to ignite during implosion when the pusher still has nearly its full implosion velocity. The high pusher-to-fuel-mass ratio M_p/M_{DT} facilitates this. The ratio of mean velocity at the time of ignition to maximum implosion velocity will be set in the design. It is termed the ignition margin parameter, $\eta_I \equiv \langle u_r(t_I) \rangle / u_I$. It can be computed analytically in the limit of a hard pusher with no internal dynamics. One can show that the implosion depends on the single parameter $\varepsilon = M_{\text{DT}}/C_*^2 M_p$, and the pusher mass (R_0 to R_1) is given by

$$M_p = \frac{M_{DT} C^2}{(1 - \eta_I^2) C_*^2} = 0.415 \frac{M_{DT}^{2/3}}{(1 - \eta_I^2)}. \quad (4)$$

For very large pusher mass $\eta_I \rightarrow 1$, Rayleigh-Taylor (RT) activity is absent. The opposite limit $\eta_I \rightarrow 0$ corresponds to ignition occurring at stagnation. This limit is superficially energy efficient and may even produce yield in 1D simulations, but has no likelihood of success in a real experiment. The hard pusher calculation will become inaccurate if applied to larger ignition margins $\eta_I > 0.9$, where pusher compressibility needs to be included. For present purposes we cite the results from the hydro-burn code simulations summarized in Fig. 2 to justify the use of Eq. (4). The pusher energy, using (3) and (4), is $E_p = E_{DT}/(1 - \eta_I^2) = 288 M_{DT}/(1 - \eta_I^2)$ kJ/mg, independent of both convergence and implosion velocity. For example, if ignition is to occur at 90% of the implosion velocity ($\eta_I = 0.9$), then for $C \sim 10$ the pusher-to-fuel-mass ratio is ~ 80 and the pusher kinetic energy is ~ 5 times the fuel internal energy. This large residual pusher energy not transferred to the fuel is the price one pays for improved margin (upstream ignition and large fractional fuel burn).

The pusher dynamic pressure $P_p = \frac{1}{2} \rho_{p0} u_I^2$, initially of order 4 Gbar is well above what can be achieved with laser ablation. Thus an additional drive shell (R_2 to R_3) will be required for pressure amplification. Simulations show that the colliding metal shells in our system can be treated as elastic collisions of masses to good accuracy. The velocity multiplication in an elastic collision is $u_I/u_d = 2/(1 + M_p/M_d)$, which implies a kinetic energy transfer

$$E_p = \eta_c E_d \frac{4x}{(1+x)^2}, \quad (5)$$

Target specs		Metric	Model	Hydra
M_{DT}	0.025	E_a	...	138.7
M_p	1.87	E_d	78.8	81.7
M_d	7.48	E_p	37.8	36.5
ρ_{bg0}	0.038	$\langle u_d \rangle$	14.5	14.80
R_0	326	$\langle u_i \rangle$	20.1	19.70
R_1	386	η_I	0.9	0.89
R_2	1107	C	9.42	9.31
R_3	1159	Y	4.21	4.29

FIG. 2. Design table for baseline target. Target specifications and metrics are from a model computed from DT mass. Comparison to HYDRA results are shown. Key data is in red. Table units are mg, μm , g/cm^3 , with shell energies in kJ, velocities in $\text{cm}/\mu\text{s}$, yield in MJ (nominal 50% burnup used for model yield).

where $x = M_p/M_d$ and η_c is a shell collision efficiency parameter, observed in simulations as $\eta_c \approx 0.75$. Choosing $M_d/M_p \equiv x^{-1} = 4$ gives, for $\eta_c \rightarrow 1$, a velocity multiplication $u_I/u_d = 1.6$ and energy transfer ratio $E_p/E_d = 0.48$.

The kinetic energy required in the drive shell is

$$E_d = \frac{588 M_{DT}}{\eta_c (1 - \eta_I^2)} \text{ kJ/mg}. \quad (6)$$

This depends only on the fuel mass and the efficiencies. For example, with $\eta_I = 0.9$, $\eta_c = 0.75$, the specific drive energy is $E_d/M_{DT} \rightarrow 4.13$ kJ/mg.

The geometry can be completed by specifying the outer radius of the drive shell which we determine by setting the convergence between shell collision as 3: $R_3 = 3R_1$. Buffer gas is needed but the density is not a critical parameter. We use DT at initial density $\rho_{bg0} = 0.5 \rho_{p0} \{ [(R_1 + 3R_0)/4]^3 - R_0^3 \} / (R_2^3 - R_1^3)$, and forgo the derivation here.

The analytic model described above computes the inner two shells' specifications and basic performance metrics as shown in Fig. 2. The underlying parameters are (1) for design, $C_* = 2.5$, $x = 0.25$, $\eta_I = 0.9$, $\eta_c = 0.75$, and $T_I = 2.5$ keV, and (2) for initial material densities (in g/cm^3) $\rho_{DT0} = 0.173$, $\rho_{p0} = 19.292$, and $\rho_{d0} = 8.938$. The ablator shell is designed using HYDRA simulations to produce the drive shell energy specified in Fig. 2. The ablator shell specs have been included Fig. 2.

The final stages of implosion and burn are shown in Fig. 3, annotated with vertical arrows to indicate the times of ignition $T_I = 2.5$ keV and peak burn. Ignition is well upstream and at nearly the velocity specified by the η_I design parameter, as shown in Fig. 2. This level of agreement has been seen for a range of targets. The pusher density is of order

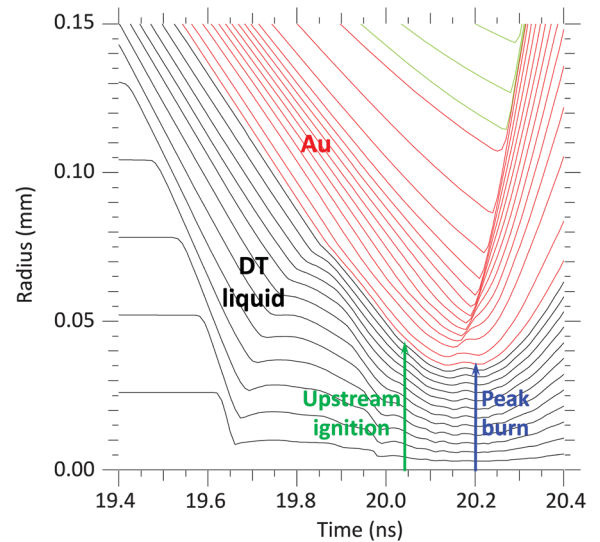


FIG. 3. Implosion diagram showing upstream ignition.

$\rho_p \approx 2000 \text{ g/cm}^3$ at the time of ignition when approximately 20% of its kinetic energy has been expended. There is a slight impulsive deceleration of the pusher when the reflected fuel shock hits it, but no continuous deceleration that would initiate Rayleigh-Taylor growth appears until after ignition. Richmeyer-Meshkov (RM) growth from the shock scales like $\sim t^{1/2}$ for the lowest saturated mode, leading to a negligible mix layer width at ignition time of order $\delta_{\text{RM}} \sim \sqrt{\delta_0 u_I t} \sim 0.6 \text{ }\mu\text{m}$, for $\sim 100 \text{ nm}$ surface perturbations. Simulations show that upstream ignition occurs when alpha heating first causes the temperature to separate from the no-burn value. Specifically, when the alpha power equals 1/4 the hydrodynamic heating rate and both are still positive (radiation is trapped by the pusher and negligible), we have upstream ignition. The ion temperature can then run away with nothing to impede the burn until temperatures are much higher and substantial yield is generated. We do not claim accurate full yield calculations, as the predictive capability does not exist. What we do have is a simple path to get to this ignition point in the laboratory (and, if necessary, to increase η_I until we do). At that point ignited fusion yield can be measured. That is the sole purpose of this design.

The ignition temperature for upstream ignition, in the past decreed to be $T_I = 2.5 \text{ keV}$ [6–11], can now be computed from the model with a numerical solution for the condition $\dot{E}_\alpha/\dot{E}_{\text{hyd}} = 1/4$, using the Bosch-Hale [17] reactivity. Taking the fuel mass from the baseline target $M_{\text{DT}} = 25 \text{ }\mu\text{g}$ gives an ignition temperature of $T_I = 2.46 \text{ keV}$. This value depends very weakly on fuel mass, so that using 2.5 keV is justified. We do not require further iterating to a fully self-consistent value.

This differs from the conventional ignition concept in which alpha heating must exceed energy losses. Because the losses depend on accurate treatments of mix, etc., which do not exist, the traditional ignition concept becomes ambiguous. Since Revolver's upstream ignition occurs sans losses, a different definition of ignition is required. The condition $\dot{E}_\alpha/\dot{E}_{\text{hyd}} = 1/4$, with no mix, is unambiguous.

Drive energy of the Revolver design is provided by a directly driven 3-mm radius, 50- μm -thick Be ablator shell that can efficiently convert a fraction of the NIF's 1.5 MJ of laser energy into inward kinetic energy. Collision between the ablator and drive shell is mediated by low density (3 mg/cm^3) DT gas between the shells. A laser power of 24 TW for 2 ns followed by 320 TW for 4.5 ns keeps the energy low during inefficient shock transit through the ablator, after which high power is used to efficiently accelerate 70% of the 10.3-mg ablator mass to $E_a = 139 \text{ kJ}$ (a total hydrodynamic efficiency of 9.3%). The use of a large radius, low convergence ablator ($C_a = 2.5$) provides additional design advantages including (a) low laser surface intensity ($I \sim 2.8 \times 10^{14} \text{ W/cm}^2$) to mitigate laser plasma instabilities [18] including cross beam energy transfer and two-plasmon decay, (b) reduced electron

temperature gradients consistent with classical local electron thermal conduction, and (c) minimal fractional change of the ablator radius during the laser pulse to minimize RT penetration of the shell and eliminate the need for laser zooming. This completes the three-shell Revolver target conceptual design.

Hydrodynamic instability growth must be addressed for Revolver as it is for all ICF implosions. The multishell configuration has additional interfaces to consider. Each shell is accelerated from its outer surface by a high-pressure lighter fluid and decelerated during collision by the pressure on its inner surface by a presumed lighter fluid, so that both surfaces of each shell are expected to induce RT activity. The mixing zone between shells is exposed to multiple reflected shocks that generate a quasi-isobaric pressure to compress the subsequent shell. It is not clear how much, if at all, mixing in these regions will affect the large-scale energy and velocity transfers. Without a predictive way to calculate the mixing we do not attempt a detailed evaluation here.

The accelerating shells must remain intact and not be penetrated through by the light side fluid bubbles of RT growth. We evaluate this effect in the limit of fully developed, self-similar growth (extensively studied for simple fluids [19,20]). For constant accelerations the mix layer growth is asymmetric about the interface and given by

$$\delta_i = \alpha_i A g t^2, \quad 1 = \text{spikes}, \quad 2 = \text{bubbles}. \quad (7)$$

For the acceleration interfaces shell penetration by the bubbles we need to evaluate δ_2 . The shell will remain intact when the penetration distance δ_2 remains smaller than the shell thickness Δ throughout the acceleration. The ratio $f_{\text{RT}} = \delta_2/\Delta$ is largest at the end of the acceleration. We evaluate the factor there. An upper bound for the similarity constant is $\alpha_2 = 0.07$ (independent of the Atwood number). This can be generalized to nonconstant g and evaluated by noting its equivalence to the fraction $2A\alpha_2 = 0.14$ of the distance traveled during acceleration. The RT penetration fractions for the three shells—ablator (a), drive (d), and pusher (p)—are

$$f_{\text{RT}}^a = 0.5, \quad f_{\text{RT}}^d = 0.57, \quad f_{\text{RT}}^p = 0.4. \quad (8)$$

These are favorable indicators for the implosion of the baseline multishell target. It is noteworthy that all existing single-shell ignition capsules evaluate poorly by this criterion with typically $f_{\text{RT}} > 2$ for the acceleration phase (see Figs. 78 and 80 of Ref. [4]). They rely on ablative stabilization to eliminate RT growth. Good performance by this measure comes from thick shells with short acceleration distances, as in the Revolver concept. Thin shells accelerated for the duration of the implosion do not show good performance.

The response of the multishell implosion to low order drive asymmetries will need to be given serious study. For

single-shell systems there are hard restrictions on the drive such that for a fuel convergence of order $C \sim 30\text{--}40$ the implosion velocity needs uniformity to order 1% [2]. The baseline target of this Letter has a net convergence of $C_{\text{net}} = 86$, which under the same scaling would require a prohibitive uniformity of laser drive. We expect the partitioned Revolver implosion to scale differently with the multiple gas shocks during a collision tending to form an isobaric gas volume that accelerates the target shell symmetrically inward. Detailed multidimensional simulation analysis is underway to determine quantitatively the size of this effect and the drive uniformity requirements.

The Revolver capsules described here are believed to be the simplest, lowest-fuel-convergence, highest-margin path to pure fusion ignition and burn. The design is focused on achieving the upstream ignition state with negligible RT growth of the pusher-fuel interface. Pusher mass is used to increase and control the ignition margin $\eta_I \equiv \langle u_r(t_I) \rangle / u_I$. We believe that reaching this ignition state will lead to high yield at the NIF. Having an experimental capability to produce and measure yield, etc., in such a configuration could open the door to a definitive solution to the long-standing quandary of mix.

The authors acknowledge useful discussions with R. C. Kirkpatrick, J. Mercer-Smith, D. J. Shirk, R. Betti, and E. M. Campbell. Work performed under the auspices of the U.S. Department of Energy by the Los Alamos National Security, LLC, Los Alamos National Laboratory under Contract No. DE-AC52-06NA25396.

-
- [1] J. H. Nuckols, L. Wood, A. Thiessen, and G. B. Zimmerman, *Nature (London)* **239**, 139 (1972).
[2] J. D. Lindl, *Phys. Plasmas* **2**, 3933 (1995).

- [3] M. J. Edwards, P. K. Patel, J. D. Lindl, L. J. Atherton, S. H. Glenzer *et al.*, *Phys. Plasmas* **20**, 070501 (2013).
[4] J. D. Lindl, O. Landen, J. Edwards, E. Moses and NIC team, *Phys. Plasmas* **21**, 020501 (2014).
[5] M. M. Marinak, G. D. Kerbel, and N. A. Gentile *et al.*, *Phys. Plasmas* **8**, 2275 (2001).
[6] R. C. Kirkpatrick, C. C. Cremer, L. C. Madsen, H. H. Rogers, and R. S. Cooper, *Nucl. Fusion* **15**, 333 (1975).
[7] R. C. Kirkpatrick and J. A. Wheeler, *Nucl. Fusion* **21**, 389 (1981).
[8] S. A. Colgate and A. G. Petschek, Los Alamos National Laboratory Report No. LA-7832, 1980.
[9] S. A. Colgate and A. G. Petschek, Los Alamos National Laboratory Report No. LA-UR-88-1268, 1988.
[10] S. A. Colgate, A. G. Petschek, and R. C. Kirkpatrick, Los Alamos National Laboratory Report No. LA-UR-92-2599, 1992.
[11] K. S. Lackner, S. A. Colgate, N. L. Johnson, R. C. Kirkpatrick, R. Menikoff, and A. G. Petschek, *AIP Conf. Proc.* **318**, 356 (1994).
[12] S. A. Colgate, W. Achison, and H. Li, Los Alamos National Laboratory Report No. LA-UR-06-3716, 2006.
[13] R. G. Watt, Los Alamos National Laboratory Report No. LA-UR-10-01981, 2010.
[14] P. Amendt, J. D. Colvin, R. E. Tipton, D. E. Hinkel, M. J. Edwards, O. L. Landen, J. D. Ramshaw, L. J. Suter, W. S. Varnum, and R. G. Watt, *Phys. Plasmas* **9**, 2221 (2002).
[15] P. Amendt, C. Cerjan, A. Hamza, D. E. Hinkel, J. L. Milovich, and H. F. Robey, *Phys. Plasmas* **14**, 056312 (2007).
[16] M. Van Dyke and A. J. Guttmann, *J. Fluid Mech.* **120**, 451 (1982).
[17] H. S. Bosch and G. M. Hale, *Nucl. Fusion* **32**, 611 (1992).
[18] J. Myatt and J. Marozas (private communication).
[19] G. Dimonte, *Phys. Plasmas* **6**, 2009 (1999).
[20] G. Dimonte, *Phys. Rev. E* **69**, 056305 (2004).